

Performance of Different Surface Incoming Solar Radiation Models and Their Impacts on Reference Evapotranspiration

Ali Mokhtari¹ · Hamideh Noory² · Majid Vazifedoust³

Received: 23 May 2017 / Accepted: 26 March 2018 /

Published online: 13 April 2018

© Springer Science+Business Media B.V., part of Springer Nature 2018

Abstract Reference evapotranspiration (ET_0) from FAO-Penman-Monteith equation is highly sensitive to the surface incoming solar radiation (SISR) and therefore accurate estimate of this parameter would result in more accurate estimation of ET_0 . In this study, the accuracy of three main approaches for SISR estimation including empirical models (Angstrom and Hargreaves-Samani), physically-based data assimilation models (Global Land Data Assimilation System-Noah, GLDAS/Noah, and National Centers of Environmental Predictions/National Center for Atmospheric Research, NCEP/NCAR), and a satellite observation model (Satellite Application Facility on Climate Monitoring, CM-SAF) were evaluated using ground-based measurements from 2012 to 2015. Then SISR outputs from introduced approaches were implemented in FAO-Penman-Monteith equation for ET_0 estimation on daily and monthly basis. The Angstrom calibrated model was the most accurate model with a coefficient of determination (R^2) of 0.9 and standard error of estimate (SEE) of $2.58 \text{ MJ} \cdot \text{m}^{-2} \cdot \text{d}^{-1}$, and GLDAS/Noah, Hargreaves-Samani, NCEP/NCAR, and CM-SAF, had lower accuracy, respectively. However, the lack of the meteorological data and required empirical coefficients are the main limitations of applying the empirical models, however, satellite-based approaches are more practical for operational purposes. The results indicated that, in spite of slight overestimation in warm months, GLDAS/Noah model had better performance with $R^2=0.87$ and $SEE = 3.5 \text{ MJ} \cdot \text{m}^{-2} \cdot \text{d}^{-1}$ in case of lack of meteorological data. The accuracy of ET_0 derived from FAO-Penman-Monteith equation was directly depended on the accuracy of SISR estimation. The ET_0 estimation error was related to SISR estimation error with a fourth-degree function and had a linear relationship with SISR error at daily and monthly scales, respectively.

✉ Hamideh Noory
hnoory@ut.ac.ir

¹ National Center for Satellite Observation, Iranian Space Agency, Alborz, Iran

² Department of Irrigation and Reclamation Engineering, University of Tehran, Tehran, Iran

³ Department of Water Engineering, University of Guilan, Rasht, Iran

Keywords Angstrom · CM-SAF · GLDAS · Hargreaves-Samani · NCEP · Reference evapotranspiration

1 Introduction

Reference evapotranspiration (ET_0) is one of the most important parameters in agro-hydrological calculations. This parameter is used in agricultural and urban management, irrigation scheduling, and studies of water balance (Ambas and Baltas 2012). ET_0 measurement is a costly and time consuming process which requires high accuracy and proficiency to conduct. Therefore, many approaches were represented based on water balance (Guitjens 1982), radiation (Priestly and Taylor 1972), combination of an energy balance and an aerodynamic formula (Penman 1948), temperature (Blaney and Criddle 1950; and Hargreaves and Samani 1985), and mass transfer (Harbeck 1962) for calculating ET_0 (Xu and Singh 2002). Combination methods consider all the possible meteorological and vegetative parameters in ET_0 calculation; therefore, they are relatively accurate compared with other approaches. Penman-Monteith is introduced as the most qualified equation in ET_0 calculation by Food and Agriculture Organization (FAO) (Allen et al. 1998). Jensen et al. (1990) evaluated 20 different evapotranspiration formulas using lysimeter data for 11 stations around the world under different climatic conditions. The Penman-Monteith formula was concluded as the most accurate for all the study areas.

Energy for evapotranspiration is provided by sun's radiation reaching the ground (surface incoming solar radiation, SISR). This energy is the source of heat and light on the earth, and it is an essential parameter in calculating evapotranspiration and many other biological processes of plants (Rosenberg et al. 1983). According to Jensen (1985), 80% of ET_0 is composed of SISR and air temperature. Therefore, an accurate estimate of SISR is highly essential in precise calculation of ET_0 .

Not all the meteorological stations are able to measure the SISR directly and also there might not be always enough meteorological data for calculating SISR, especially in outlying agricultural fields. Hence, determining accurate SISR in areas with the lack of ground measured data has always been a big challenge for researchers, which is why finding an alternative to station-based data for such cases would be helpful. There is no accepted methodology for classifying the SISR models (Gueymard and Myers 2008); however, Bojanowski (2013) categorized this parameter into four different ways: (Abraha & Savage, 2008) ground measurement (Aghashariatmadari, 2011) empirical models (Aladenola & Madramootoo, 2014) physically-based models (Allen, 1995) satellite observation models.

Ground measurement is the most accurate approach for determining SISR, which is conducted using the pyranometers to measure the horizontal beam and diffuse irradiances (global irradiance) (Paulescu et al. 2013). Some types of pyranometers are invalid for measuring reflected radiation due to the difference in spectral response between the instruments and reflecting surface (Allen et al. 2005). Therefore, because of the high sensitivity of these devices, they need constant care and calibration (Ohmura et al. 1998). Which is why SISR measurement is a costly and also time consuming process, and there are few meteorological stations that are able to do this.

Empirical models are developed based on the relationship between SISR and various meteorological data, which directly or indirectly represents the cloudiness. The cloudier the sky the less solar radiation reaches the ground. Daily sunshine hours and air temperature are the basis for empirical models such as Angstrom model (Angstrom 1924) and Hargreaves-

Samani model (Hargreaves and Samani 1982), respectively. Daily sunshine hours is not measured in every meteorological station, so the temperature-based approach would be an appropriate alternative for calculating SISR in these cases. The biggest limitations of empirical models are their area-dependant empirical coefficients (Abraha and Savage 2008). Therefore, the accurate calibration of these models is often not possible due to the lack of meteorological data. Bojanowski et al. (2013) in Europe, Aladenola and Madramootoo (2014) in Canada, Liu et al. (2014) in three different regions with three different climatic conditions in China, and Piri and Kisi (2015) in two different climatic conditions in Iran showed that the calibrated Angstrom model outperform the Hargreaves-Samani model.

Physically-based models estimate SISR using the radiative transfer models and satellite-based data including the physical characteristics of the earth's surface, atmosphere, and clouds (Inamdar and Guillevic 2015). The Land Surface Models (LSMs) are the means of simulating interactions between land surface and atmosphere (Rodell et al. 2004). In order to calculate SISR, these models consider environmental parameters such as cloudiness, aerosol type and thickness, amount of water vapor in atmosphere, thickness of ozone layer, and depth of snow that covers the surface (Rodell et al. 2004, Schulz et al. 2009). Since there are not always enough observation data in every study area, and also because of limited understanding about all the natural processes that occurs on the earth, data assimilation technique is utilized in order to augment the models with measurement and satellite observations to improve estimations and weather forecasting. In addition, the uncertainty of input data in models would be significantly suppressed (Zhang and Pu 2010). The data assimilation is being done using ground or satellite-based observations; therefore, it is not possible to completely separate the physically-based models from satellite observation models. The National Centers of Environmental Predictions [NCEP, formerly known as the National Meteorological Center, (NMC)]/National Center for Atmospheric Research (NCAR) reanalysis project began in 1991 with the aim to observe climate changes using the Global Data Assimilation System (GDAS). The NCEP/NCAR reanalysis uses a frozen state-of-the-art global data assimilation system and a complete database for calculating daily SISR (Kalnay et al. 1996). The North American Land Data Assimilation System (NLDAS) project merges the LSMs with observational data from disparate measurement systems as a complementary in order to fill the gaps. The Global Land Data Assimilation System (GLDAS) is the outgrowth of NLDAS (Rodell et al. 2004) which takes into account the satellite-based and ground-based data sets for modeling the SISR globally. These models have coarse spatial resolution in field scale applications which in some cases results in an inaccurate estimations of SISR; accordingly, Babst et al. (2008) showed that the NCEP accuracy is limited on a regional scale. Also, Wang et al. (2011) studied the GLDAS-based SISR with spatial resolution equal to 0.25 degree in two different climatic conditions in China. They showed that the GLDAS overestimates the SISR compared to the measured SISR; therefore, they used a correction factor to ameliorate the GLDAS-based SISR estimation.

There are many sensors onboard different satellites for SISR estimation, such as Earth Radiation Budget (ERB) onboard the NIMBUS-7 (Jacobowits and Tighe 1984), Clouds and the Earth's Radiant Energy System (CERES) onboard the Terra, Aqua, and TRMM satellites (Barkstrom and Smith 1986), Geostationary Earth's Radiation Budget (GERB) onboard Meteosat-8 and Meteosat-9 (Harries et al. 2005), Spinning Enhanced Visible and Infrared Imager (SEVIRI) onboard the METEOSAT second generation (MSG) and GOES-R ABI satellites (Laszlo et al. 2008), Moderate Resolution Imaging Spectroradiometer (MODIS) onboard Terra and Aqua (Liang et al. 2006), Earth's Radiation Budget Experiment (ERBE) sensors, which are carried by the ERBS, NOAA-9, and NOAA-10 satellites (Barkstrom et al. 1989; Barkstrom et al. 1990), Scanner for Radiative Budget (ScaRaB) onboard the Russian

satellites named Meteor-3-7 and Resurs-1 (Kandel et al. 1998; Duvel et al. 2001), Meteosat Visible and Infrared Imager (MVIRI) onboard the METEOSAT first generation (MFG) satellite, and many other sensors onboard the various other geostationary satellites (GMS, INDOEX, GOES E and GOES W). Geostationary satellites are placed directly over the equator that revolves in the same direction the earth rotates (west to east). Therefore, the temporal resolution of these satellites is much higher than the polar orbiting satellites (e.g. GOES R and W satellites are able to scan the earth in every one minute) which leads to the more precise estimations of SISR. However, these satellites are not able to cover the earth uniformly in terms of spatial resolution. SISR estimations of the satellite observation models are based on establishing a relationship between the top of atmosphere reflectance - which represents the cloudiness - and SISR (Cano et al. 1986). Obtaining this information from satellites is always accompanied by unintended uncertainties. Satellite Application Facility on Climate Monitoring (CM-SAF) (Hollman et al. 2006) is a satellite observation model and a consistent dataset of cloud and radiation products in a high spatial resolution on a uniform grid. The CM-SAF is dedicated to produce climate datasets using data from instruments onboard of METEOSAT Second Generation and polar orbiting satellites NOAA and METOP.

The objective of this study is to investigate the performance of SISR derived from two empirical models based on sunshine hours (Angstrom) and daily air temperature (Hargreav-Samani), two physically-based data assimilation models (GLDAS/Noah and NCEP/NCAR), and a satellite observation model (CM-SAF) in ET_0 calculation using FAO-Penman-Monteith equation and also find an alternative to measured data, considering their accuracy and more importantly their limitations and restrictions.

2 Materials and Methods

2.1 Study Area

The study area is located in the Qazvin irrigation network. The Qazvin plain is a semi-arid region with 250 mm precipitation and 2200 mm evaporation annually. Those pixels covering the Qazvin synoptic station were used in this study. The meteorological data was acquired from the Qazvin station (Table 1), which stands in latitude 36.26 N degrees and longitude 50.06 E degrees (Fig. 1).

2.2 The Surface Solar Radiation Models

2.2.1 Empirical Models

Two empirical SISR estimation models were evaluated in this study. One based on daily sunshine hours and the other model takes air temperature into account. Angstrom (1924) showed that the SISR has a strong relationship with daily sunshine hours and extraterrestrial solar radiation (Eq. 1).

$$R_s = \left(a_s + b_s \cdot \frac{n}{N} \right) R_a \quad (1)$$

where R_a = extraterrestrial solar radiation ($\text{MJ} \cdot \text{m}^{-2} \cdot \text{d}^{-1}$); n = daily sunshine hours (hr); N = daylight duration (hr); a_s and b_s = empirical coefficients (dimensionless). These two coefficients

Table 1 Datasets specifications used in this study

| Data | Source | Product Name | Spatial Resolution | Temporal Resolution | Acquisition Date |
|----------------------|--|---|-----------------------------|---------------------|---------------------------|
| Meteorological Data | Qazvin station | Surface Incoming Solar Radiation (MJ.m^{-2}) | – | Hourly | 1-Jan-2012 to 31-Dec-2015 |
| | | Sunshine Hours (hrs) | – | Hourly | |
| | | Minimum & Maximum Temperature ($^{\circ}\text{C}$) | – | Hourly | |
| | | Minimum & Maximum Relative Humidity (%) | – | Hourly | |
| | | Wind Speed (m.s^{-1}) | – | Hourly | |
| | | Rain (mm) | – | Hourly | |
| DEM | earthexplorer.usgs.gov | – | 30×30 (meter) | – | – |
| GLDAS/Noah | mirador.gsfc.nasa.gov | GLDAS_NOAH025SUBP_3H | 0.25×0.25 (degree) | 3 Hourly | 1-Jan-2012 to 31-Dec-2015 |
| NCEP/NCAR Reanalysis | esrl.noaa.gov | Downward Solar Radiation Flux | 0.94×0.94 (degree) | Diurnal | 1-Jan-2012 to 31-Dec-2015 |
| CM-SAF | cmsaf.eu | SIS - Surface Incoming Shortwave Radiation | 15×15 (Kilometer) | Diurnal | 1-Jan-2012 to 31-Dec-2015 |

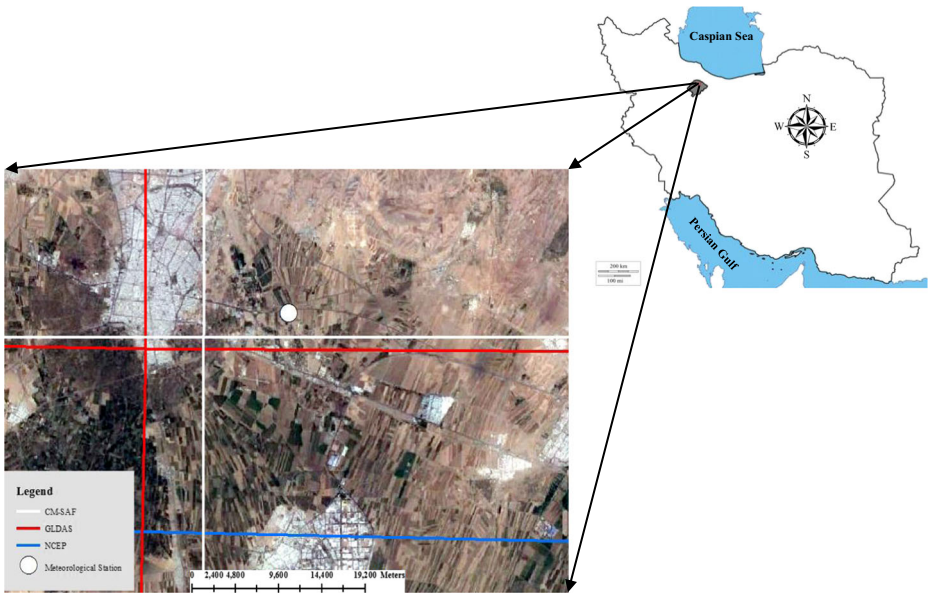


Fig. 1 Satellite SISR products including GLDAS/Noah, NCEP/NCAR, and CM-SAF pixels locations superimposed over the study area. The white dot is Qazvin synoptic meteorological station

are usually set to 0.25 and 0.5, respectively when there are not enough data for model calibration (Allen 1997). In this study, the calibrated coefficients presented in Aghashariatmadari (2011) were taken into account, which was 0.155153 and 0.60906 for a_s and b_s , respectively.

Hargreaves and Samani (1982) calculated the SISR using the difference between the maximum and minimum daily air temperature (Eq. 2). Therefore, this approach could be more operational in areas with the lack of daily sunshine hours (Aladenola and Madramootoo. 2014).

$$R_s = K_r(T_{\max} - T_{\min})^{0.5} R_a \quad (2)$$

where T_{\max} and T_{\min} = maximum and minimum air temperature respectively ($^{\circ}\text{C}$); Allen suggested calculating K_r as:

$$K_r = K_{ra} \left(\frac{P}{P_0} \right)^{0.5} \quad (3)$$

where P and P_0 = mean atmospheric pressure at the site and at sea level respectively (kPa); K_{ra} = empirical coefficient which is considered 0.2 for coastal regions and usually set to 0.17 for non-coastal regions (Samani et al. 2007). R_a is the extraterrestrial radiation calculated using Duffie and Beckman (1980, 1991) method.

2.3 Satellite-Based Models

2.3.1 Physically-Based Models

Global Land Data Assimilation System (GLDAS) GLDAS makes use of four advanced LSMs such as Noah (Chen et al. 1996; Betts et al. 1997; Koren et al. 1999; Ek et al. 2003), Mosaic (Koster and Suarez 1992), the Community Land Model (CLM) (Dai et al. 2003), and

Variable Infiltration Capacity model (VIC) (Liang et al. 1994). In this study, the GLDAS/Noah LSM with a spatial resolution of 0.25×0.25 degrees and a temporal resolution of 3 h subsetting product (Table 1) was used, which makes use of the new generation of ground and space-based observation systems to estimate the weather data more accurately (Rodell et al. 2004). The SISR calculation algorithm is presented in Shapiro (1972).

National Centers of Environmental Predictions/National Center for Atmospheric Research (NCEP/NCAR) Reanalysis NCEP/NCAR Reanalysis data is available from 1948 till present. GDAS is the operational atmospheric data assimilation system of NCEP (Derber et al. 1991). The temporal resolution is daily with a spatial resolution of 0.94×0.94 degrees for daily SISR (Table 1). The observation data which was assimilated into NCEP/NCAR's LSM includes temperature, wind, specific humidity, and surface pressure (Kistler et al. 2001).

2.4 Satellite Observation Models

The CM-SAF makes use of a well-validated algorithm to calculate surface radiation budget. Four disparate components including SISR, Surface Downwelling Longwave Radiation, Surface Outgoing Longwave Radiation, and Surface Albedo are derived. After calculating the surface radiation budget, the satellite-derived cloud module is applied. A complete description of the algorithm is presented in Dybbroe et al. (2000a, b).

2.5 Reference Evapotranspiration (ET_0) Calculation

ET_0 varies with the magnitude of error in input meteorological data. Several studies were done analyzing the sensitivity of many forms of the Penman-Monteith equation to climatic variables such as radiation, air temperature, air humidity, and wind speed which are the key parameters in ET_0 calculation. These variables affect Penman-Monteith- ET_0 in each climatic condition differently; therefore, prioritizing these variables based on their sensitivity is not absolutely possible. However, radiation was ranked as one of the most sensitive component of the Penman-Monteith equation (Goyal 2004; Gong et al. 2006; Wang et al. 2007; Bakhtiari and Liaghat 2011; Sharifi and Dinpashoh 2014).

In this study, the FAO-Penman-Monteith equation (Eq. 4) was used to calculate daily ET_0 .

$$ET_0 = \frac{0.408\Delta(R_n - G) + \gamma \frac{900}{T + 273} u_2 (e_s - e_a)}{\Delta + \gamma(1 + 0.34u_2)} \quad (4)$$

Where R_n =Surface net radiation ($\text{MJ. m}^{-2}. \text{d}^{-1}$); G =soil heat flux density ($\text{MJ. m}^{-2}. \text{d}^{-1}$); γ = psychrometric constant ($\text{kPa. } ^\circ\text{C}^{-1}$); T = mean daily air temperature at 2 m height ($^\circ\text{C}$); u_2 = wind speed at 2 m height (m. s^{-1}); e_s = saturation vapor pressure (kPa); e_a = actual vapor pressure (kPa); Δ = slope vapor pressure curve ($\text{kPa. } ^\circ\text{C}^{-1}$).

R_n is estimated using the income and outcome radiation equilibrium at the ground level (Eq. 5).

$$R_n = (1 - \alpha)R_s + \text{RL}\downarrow - \text{RL}\uparrow - (1 - \varepsilon_0)\text{RL}\downarrow \quad (5)$$

where α =Surface albedo (dimensionless); R_s =Surface incoming solar radiation, SISR, ($\text{MJ. m}^{-2}. \text{d}^{-1}$); $\text{RL}\downarrow$ =Incoming downwelling longwave radiation, SDLR, ($\text{MJ.m}^{-2}.\text{d}^{-1}$); $\text{RL}\uparrow$ =Outgoing longwave radiation ($\text{MJ. m}^{-2}. \text{d}^{-1}$); ε_0 =Surface emissivity (dimensionless).

Daily ET_0 was calculated using each SISR model for four consecutive years from 2012 to 2015.

2.6 Datasets

The meteorological data and satellite products specifications are mentioned in Table 1. Measured SISR, which was used for evaluating the SISR models and calculating ET_0 using the FAO-Penman-Monteith equation, was measured from calibrated and well maintained pyranometers in the Qazvin synoptic station.

2.7 Accuracy Analysis

The accuracy of estimated SISR was evaluated using the coefficient of determination (R^2) which represents the dispersion of the points from regression line and the standard error of estimate (SEE). The SEE which is the measure of the accuracy of prediction was calculated as follows:

$$SEE = \sqrt{\frac{\sum(Y_r - Y_p)^2}{n-1}} \quad (6)$$

Where Y_r and Y_p = measured and predicted value respectively; n = number of observations.

3 Results and Discussion

3.1 Surface Incoming Solar Radiation (SISR) Models Evaluation

3.1.1 Empirical Models

SISR output of the Angstrom and Hargreaves-Samani models were analyzed against measured data (Fig. 2). Since there were enough meteorological data to calibrate these models, they were able to estimate SISR accurately.

Both models estimated SISR with high accuracy. However, due to the fact that the Angstrom calibrated model makes use of sunshine hours data, which directly represents the

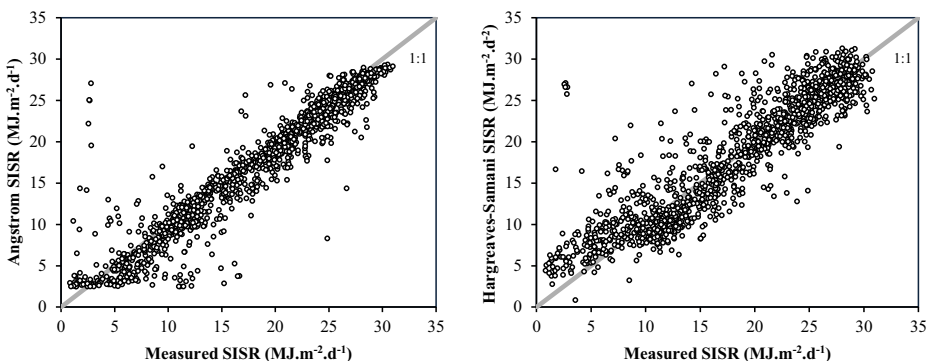


Fig. 2 Evaluation of Angstrom, Hargreaves-Samani daily SISR output from 2012 to 2015

Table 2 The evaluation indices for daily and monthly SISR derived from Angstrom, Hargreaves-Samani, GLDAS/Noah, and NCEP/NCAR models

| | | R2 | | SEE (MJ. m ⁻²) | | Mean (MJ. m ⁻²) | | Difference (MJ. m ⁻²) | |
|------------------|-------------------|-------|---------|----------------------------|---------|-----------------------------|---------|-----------------------------------|---------|
| | | Daily | Monthly | Daily | Monthly | Daily | Monthly | Daily | Monthly |
| Measured | Pyranometer | – | – | – | – | 18.04 | 540.32 | 0 | 0 |
| Empirical | Angstrom | 0.90 | 0.988 | 2.58 | 28.60 | 17.21 | 522.54 | -0.84 | -17.78 |
| | Hargreaves-Samani | 0.83 | 0.967 | 3.23 | 42.59 | 18.11 | 550.03 | 0.07 | 9.71 |
| Satellite -based | GLDAS/Noah | 0.87 | 0.989 | 3.50 | 71.36 | 19.88 | 603.50 | 1.83 | 63.18 |
| | NCEP/NCAR | 0.83 | 0.977 | 4.46 | 105.93 | 20.99 | 637.34 | 2.95 | 97.02 |
| | CM-SAF | 0.53 | – | 11.84 | – | 18.29 | – | 0.24 | – |

cloudiness, had higher accuracy compared to the Hargreaves-Samani model (Table 2). According to Table 2, the R² of the Angstrom and Hargreaves-Samani models were 0.9 and 0.83, respectively, and the SEE was 2.58 MJ. m⁻² for the Angstrom model and 3.23 MJ. m⁻² for the Hargreaves-Samani model. But, in spite of lower efficiency of Hargreaves-Samani model, this model is relatively more practical in areas with unmeasured sunshine hours. Monthly evaluation of SISR derived from empirical models showed that the dispersion of the points decreased (Fig. 3) and R² significantly increased for monthly SISR compared to daily SISR (Table 2). Similar to daily SISR evaluation, Angstrom model was slightly underestimating this parameter in most of the months (Table 3). The overestimation of SISR resulted from the Hargreaves-Samani model was negligible, but the SEE was higher compared to the Angstrom model (Table 2).

3.1.2 Satellite-Based Models

According to Fig. 4 and Table 2, all satellite-based products overestimated daily and monthly SISR.

SISRs derived from GLDAS/Noah, NCEP/NCAR, and CM-SAF were overestimated about 10, 16, and 1% at daily scale and SISRs of GLDAS/Noah and NCEP/NCAR models were also overestimated about 11.5 and 18% at monthly scale, respectively (Table 2). CM-SAF-derived SISR product does not cover all the earth in each data presentation, which results in a lack of

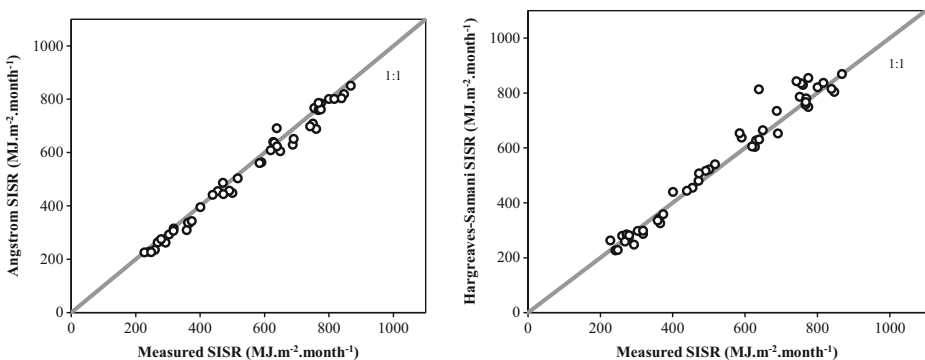


Fig. 3 Monthly SISR for empirical models (Angstrom and Hargreaves-Samani) from 2012 to 2015

Table 3 Four-year monthly average and differences from measured surface incoming solar radiation (SISR) of Angstrom, Hargreaves-Samani, GLDAS/Noah, and NCEP/NCAR models for each month from 2012 to 2015

| Month | Measured (MJ. m ⁻² . month ⁻¹) | Angstrom (MJ. m ⁻² . month ⁻¹) | | Hargreaves-Samani (MJ. m ⁻² . month ⁻¹) | | GLDAS/Noah (MJ. m ⁻² . month ⁻¹) | | NCEP/NCAR (MJ. m ⁻² . month ⁻¹) | |
|-----------|--|---|------------|--|------------|---|--------------|--|--------------|
| | | Observed | Difference | Observed | Difference | Observed | Difference | Observed | Difference |
| January | 121.66 | 116.08 | -5.58 | 117.20 | -4.46 | 135.52 | 13.86 | 147.99 | 26.32 |
| February | 148.17 | 133.60 | -14.57 | 137.46 | -10.71 | 160.46 | 12.29 | 177.50 | 29.33 |
| March | 200.75 | 187.14 | -13.61 | 210.66 | 9.91 | 224.90 | 24.15 | 252.91 | 52.17 |
| April | 254.84 | 240.54 | -14.30 | 263.46 | 8.62 | 281.59 | 26.75 | 303.36 | 48.52 |
| May | 285.54 | 275.71 | -9.84 | 321.06 | 35.52 | 327.66 | 42.12 | 355.34 | 69.80 |
| June | 326.24 | 310.62 | -15.62 | 333.86 | 7.62 | 367.38 | 41.14 | 377.15 | 50.92 |
| July | 328.16 | 325.41 | -2.76 | 339.77 | 11.60 | 369.92 | 41.76 | 376.11 | 47.94 |
| August | 311.80 | 312.62 | 0.82 | 308.48 | -3.32 | 342.86 | 31.06 | 354.60 | 42.80 |
| September | 254.91 | 253.55 | -1.36 | 249.03 | -5.87 | 276.63 | 21.73 | 284.39 | 29.48 |
| October | 179.03 | 179.65 | 0.62 | 183.52 | 4.49 | 202.85 | 23.82 | 209.50 | 30.46 |
| November | 107.33 | 104.90 | -2.43 | 111.03 | 3.70 | 124.62 | 17.29 | 130.49 | 23.16 |
| December | 106.61 | 98.87 | -7.74 | 96.70 | -9.90 | 117.57 | 10.96 | 127.06 | 20.45 |

*Bold values are indicative of highly overestimated SISR of a month

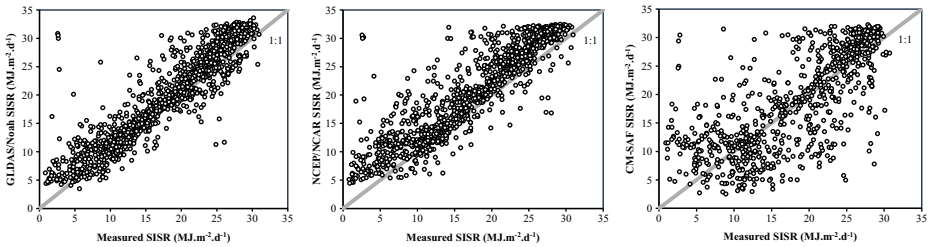


Fig. 4 Daily SISR for three satellite-based models (GLDAS/Noah, NCEP/NCAR, and CM-SAF) against measured SISR from 2012 to 2015

data for all the days around the year. Therefore, calculating monthly CM-SAF-based SISR was not possible.

Daily GLDAS/Noah-based SISR with $R^2=0.87$ and $SEE = 3.5 \text{ MJ} \cdot \text{m}^{-2} \cdot \text{d}^{-1}$ at daily time scale and with $R^2=0.989$ and $SEE = 71.36 \text{ MJ} \cdot \text{m}^{-2} \cdot \text{month}^{-1}$ at monthly scale was the most efficient among the satellite-based products and the second best among all the models. On the other hand, CM-SAF with $R^2=0.53$ and $SEE = 11.84 \text{ MJ} \cdot \text{m}^{-2} \cdot \text{d}^{-1}$ was the least accurate model at daily scale. GLDAS/Noah model is considered the advanced version of NCEP/NCAR. NCEP/NCAR model only makes use of GDAS to calculate SISR. In other hands, in addition to an atmospheric data assimilation system, GLDAS/Noah calculates SISR considering the cloud and snow products from the Air Force Weather Agency's Agricultural Meteorology Modeling System. Therefore, the advantage of the GLDAS/Noah-derived SISR against NCEP/NCAR-derived SISR is the use of satellite-based cloud cover, as opposed to the model-based cloud cover used in the radiation calculations of the atmospheric data assimilation systems (Rodell et al. 2004), and higher spatial resolution. According to the fact that data assimilation technique and satellite and ground-based observation data are not used in SISR calculation by CM-SAF, it had lower accuracy than GLDAS/Noah- and NCEP/NCAR-based SISR. CM-SAF takes into account only the relationship between the broadband atmospheric transmittance (0.2 to 0.4 μm) and the top of atmosphere reflectance to estimate SISR (Hollman et al. 2006).

The monthly SISR derived from all the satellite-based models except CM-SAF against measured SISR are depicted in Fig. 5. Results showed that the satellite-based monthly SISR are also overestimated, which the overestimation is more considerable in NCEP/NCAR model.

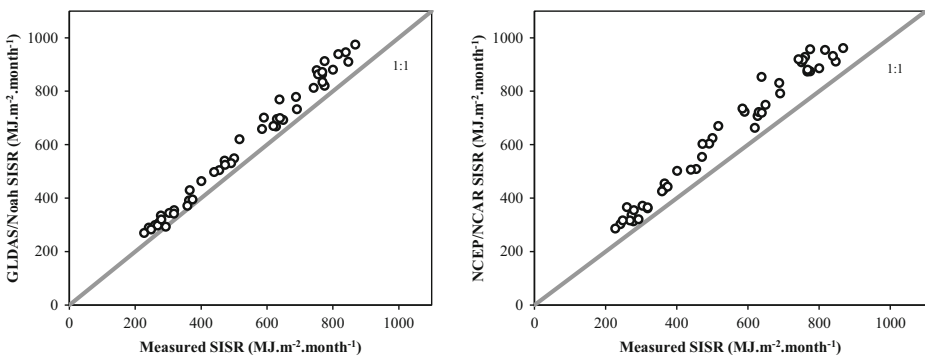


Fig. 5 Monthly SISR for two satellite-based models (GLDAS/Noah, and NCEP/NCAR) models from 2012 to 2015

Numerical comparisons of four-year average of SISR for each month showed that there are larger differences in warm months from May to July for GLDAS/Noah model and from March to August for NCEP/NCAR model (Table 3).

3.1.3 Impact of SISR Output on ET_0

ET_0 was calculated via REF_ET software (Allen 2000) using the FAO-Penman-Monteith equation for SISR derived from the Angstrom, Hargreaves-Samani, GLDAS/Noah, and NCEP/NCAR models (Fig. 6).

The lack of diurnal SISR of CM-SAF output made it inefficient in ET_0 calculation. Therefore, the CM-SAF-based SISR was ignored at daily and monthly scales. Daily ET_0 was highly depended on daily fluctuations of SISR. The accuracy of ET_0 decreased with the decrease in SISR estimation accuracy. Similar to the SEE evaluation of SISR (Table 2), the SEE increased respectively for ET_0 calculated from Angstrom, Hargreaves-Samani, GLDAS/Noah, and NCEP/NCAR-based SISR at both daily and monthly scales (Table 4).

The SEE was very low in both daily and monthly ET_0 compared to SISR (Figs. 4 and 5), because the dispersion was suppressed due to the use of many other parameters other than SISR including air temperature, wind speed, and air humidity which are also the key input data for the FAO-Penman-Monteith equation. The Angstrom model with $R^2=0.987$ and $SEE = 0.27$ mm. d⁻¹ had the best estimate for daily ET_0 . GLDAS/Noah was the second best model in ET_0 calculation with SEE and R^2 equal to 0.39 mm. d⁻¹ and 0.981, respectively, which was a reliable model for ET_0 calculation. It also had the best efficiency among the satellite products.

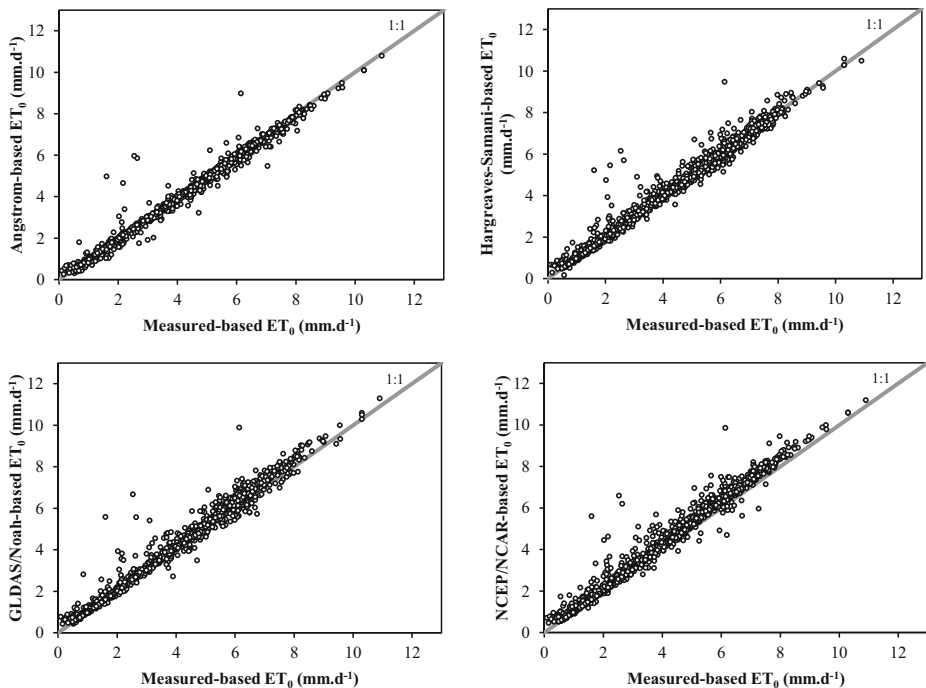


Fig. 6 Evaluation of daily ET_0 calculated from Angstrom, Hargreaves-Samani, GLDAS/Noah, NCEP/NCAR, and CM-SAF SISR output from 2012 to 2015

Table 4 The evaluation indices of daily and monthly ET_0 calculated using SISR derived from Angstrom, Hargreaves-Samani, GLDAS/Noah, and NCEP/NCAR models from 2012 to 2015

| | R^2 | | SEE (mm) | | Mean (mm) | | Difference (mm) | |
|-------------------|-------|---------|----------|---------|-----------|---------|-----------------|---------|
| | Daily | Monthly | Daily | Monthly | Daily | Monthly | Daily | Monthly |
| Measured | – | – | – | – | 3.70 | 110.94 | 0 | 0 |
| Angstrom | 0.987 | 0.999 | 0.27 | 2.93 | 3.64 | 109.20 | -0.06 | -1.73 |
| Hargreaves-Samani | 0.979 | 0.996 | 0.34 | 4.40 | 3.75 | 112.28 | 0.04 | 1.34 |
| GLDAS | 0.981 | 0.998 | 0.39 | 7.39 | 3.89 | 116.52 | 0.19 | 5.58 |
| NCEP | 0.979 | 0.997 | 0.46 | 10.20 | 3.97 | 119.00 | 0.27 | 8.06 |

Using GLDAS/Noah and NCEP/NCAR in ET_0 calculation resulted in slight overestimation of ET_0 for about 5 and 7% at both daily and monthly scales, respectively (Table 4).

The ET_0 evaluation of four consecutive years, from 2012 to 2015, are illustrated in Fig. 7. Similar to monthly SISR, an overestimation in ET_0 calculated using GLDAS/Noah and NCEP/NCAR-based SISR products was observed (Fig. 7) especially in warm months from May to July and from April to August, respectively (Table 5), although this overestimation was suppressed due to the use of many other effective parameters in FAO-Penman-Monteith- ET_0 calculation. The underestimation of ET_0 calculated using Angstrom-based SISR was very low and negligible.

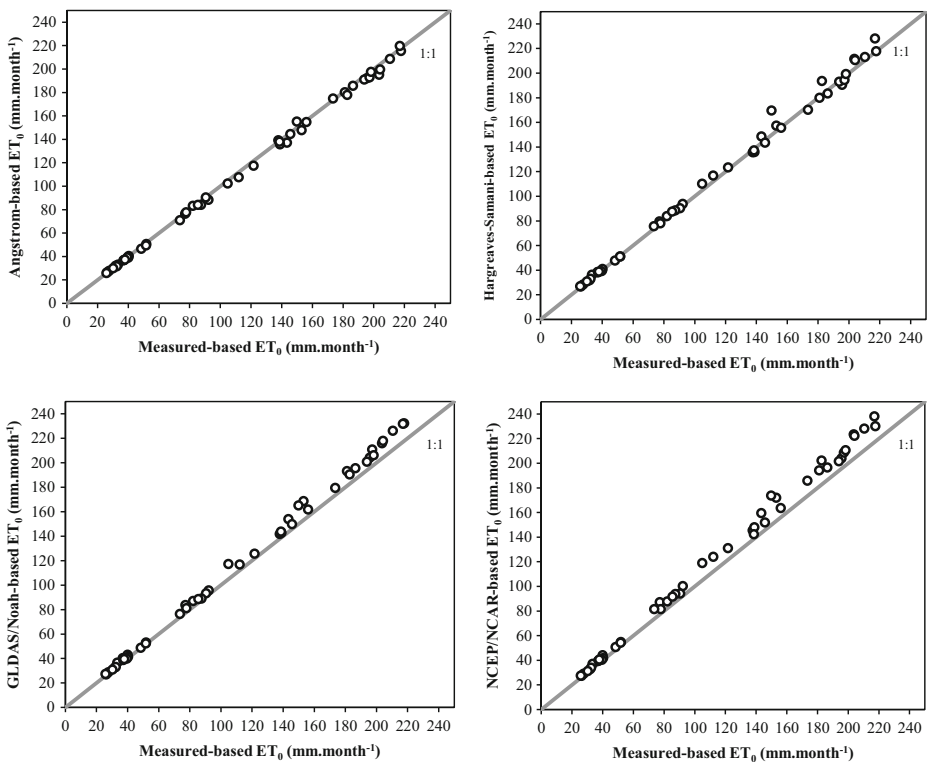


Fig. 7 Monthly ET_0 for measured, Angstrom, Hargreaves-Samani, GLDAS/Noah, and NCEP/NCAR SISR output from 2012 to 2015

Table 5 Four-year monthly average and differences from measured SISR-based reference evapotranspiration (ET₀) of Angstrom, Hargreaves-Samani, GLDAS/Noah, and NCEP/NCAR SISR-based ET₀ for each month from 2012 to 2015

| Month | Measured (mm/month) | | Angstrom (mm/month) | | Hargreaves-Samani (mm/month) | | GLDAS/Noah (mm/month) | | NCEP/NCAR (mm/month) | |
|-----------|---------------------|------------|---------------------|------------|------------------------------|------------|-----------------------|--------------|----------------------|--------------|
| | Calculated | Difference | Calculated | Difference | Calculated | Difference | Calculated | Difference | Calculated | Difference |
| January | 36.10 | -0.46 | 35.64 | -0.46 | 36.05 | -0.05 | 36.68 | 0.58 | 37.10 | 1.01 |
| February | 48.06 | -1.80 | 46.26 | -1.80 | 47.26 | -0.80 | 49.17 | 1.10 | 50.82 | 2.76 |
| March | 82.69 | -2.83 | 79.86 | -2.83 | 84.19 | 1.50 | 86.05 | 3.36 | 90.54 | 7.85 |
| April | 119.44 | -3.83 | 115.61 | -3.83 | 121.44 | 2.00 | 125.43 | 5.99 | 130.38 | 10.94 |
| May | 157.32 | -2.94 | 154.39 | -2.94 | 167.15 | 9.82 | 169.36 | 12.03 | 176.71 | 19.38 |
| June | 200.25 | -5.40 | 194.85 | -5.40 | 201.64 | 1.40 | 212.07 | 11.82 | 214.43 | 14.18 |
| July | 209.87 | -1.32 | 208.55 | -1.32 | 212.86 | 2.99 | 222.56 | 12.69 | 224.34 | 14.47 |
| August | 184.90 | -0.47 | 184.42 | -0.47 | 183.12 | -1.78 | 193.38 | 8.48 | 196.64 | 11.74 |
| September | 144.61 | -0.64 | 143.96 | -0.64 | 142.87 | -1.74 | 149.13 | 4.52 | 150.75 | 6.14 |
| October | 84.03 | -0.35 | 83.68 | -0.35 | 84.84 | 0.81 | 87.35 | 3.32 | 88.68 | 4.65 |
| November | 36.44 | -0.57 | 35.87 | -0.57 | 37.84 | 1.40 | 38.64 | 2.20 | 39.00 | 2.56 |
| December | 27.55 | -0.19 | 27.36 | -0.19 | 28.07 | 0.52 | 28.40 | 0.85 | 28.61 | 1.07 |

*Bold values are indicative of highly overestimated ET₀ of a month

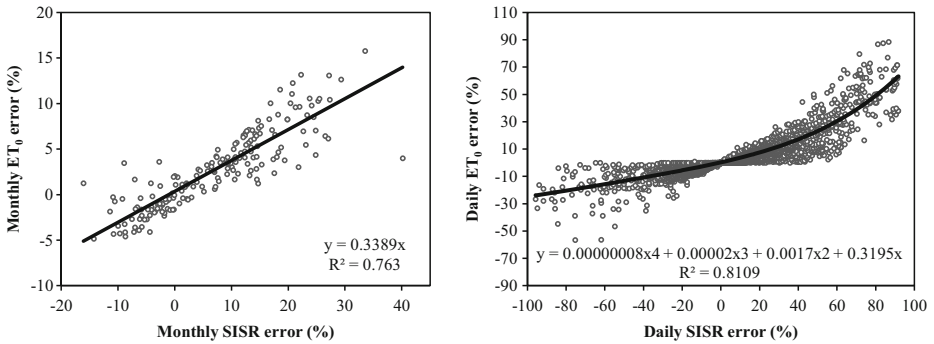


Fig. 8 Daily and monthly error percentage evaluation of SISR and ET_0 for four consecutive years from 2012 to 2015

The impact of SISR estimation on ET_0 calculation using the FAO-Penman-Monteith equation was evaluated at daily and monthly scales and results are shown in Fig. 8.

Results indicated that daily ET_0 estimation error was related to daily SISR estimation error with a fourth-degree equation. In this case, the error rate of ET_0 calculation depends on how much overestimation or underestimation is occurred in daily SISR calculation. For example, 20% overestimation and 20% underestimation of daily SISR resulted in approximately 7.24% overestimation and 5.85% underestimation of daily ET_0 , respectively. Results also showed that the error in SISR estimation affects FAO-Penman-Monteith- ET_0 linearly at monthly scale. It is implied that regardless of error rate, the error made by SISR estimation in ET_0 calculation was 0.3389 times of monthly SISR estimation error. For example, 20% overestimation of monthly SISR resulted in approximately 6.788% overestimation of monthly ET_0 .

In principle, the accuracy of empirical models is limited to the fields close to a meteorological station. Therefore, in areas with no available measured SISR, the calibration of empirical models is not possible accurately. Thus, according to the high sensitivity of the FAO-Penman-Monteith equation to SISR, ET_0 calculation would result in too much error. Results showed that, in such areas, the GLDAS/Noah SISR product, which was the most efficient model among the satellite products, would be more practical and accurate compared to empirical models in ET_0 calculation using the FAO-Penman-Monteith equation.

4 Conclusions

Because of the high sensitivity of the FAO-Penman-Monteith equation to radiation parameter, a reliable estimation of SISR is necessary to properly calculate ET_0 . In this study, daily and monthly SISR derived from two empirical models (Angstrom and Hargreaves-Samani) and three satellite products (GLDAS, NCEP, and CM-SAF) were evaluated. Also, their impacts on daily and monthly FAO-Penman-Monteith- ET_0 were discussed. Results showed that Angstrom calibrated model was the most accurate among all the models, and Hargreaves-Samani could be an alternative for areas with the lack of daily sunshine hours. It is undeniable that these models are limited to areas close to a meteorological station. Therefore, in spite of slight overestimation of SISR especially in warm months, GLDAS/Noah SISR product, which was the second best model in both daily and monthly SISR estimation, was presented as an appropriate alternative in areas with the lack of measured SISR data. The accuracy of daily and monthly ET_0 from the FAO-Penman-Monteith equation was directly related to the

accuracy of daily and monthly SISR. Results indicated that ET_0 estimation error was related to SISR estimation error with a quartic function and had a linear relationship with SISR error at daily and monthly scales, respectively. In the end, this concept was implied that the GLDAS/Noah model would be beneficial for ET_0 calculation using the FAO-Penman-Monteith equation in areas with unmeasured or poorly measured SISR.

References

- Abraha MG, Savage MJ (2008) Comparison of estimates of daily solar radiation from air temperature range for application in crop simulations. *Agric For Meteorol* 148(3):401–416
- Aghashariatmadari Z (2011) Evaluation of different models for estimating total solar radiation at horizontal surfaces based on meteorological data, with emphasis on the performance of the angstrom model over Iran. Dissertation, University of Tehran (IN PERSIAN)
- Aladenola OO, Madramootoo CA (2014) Evaluation of solar radiation estimation methods for reference evapotranspiration estimation in Canada. *Theor Appl Climatol* 118(3):377–385
- Allen RG (1995) Evaluation of procedures for estimating mean monthly solar radiation from air temperature. Report submitted to the United Nations Food and Agricultural Organization (FAO), Rome Italy
- Allen RG (1997) Self-calibrating method for estimating solar radiation from air temperature. *J Hydrol Eng* 2(2): 56–67
- Allen RG (2000) REF-ET: reference evapotranspiration calculation software for FAO and ASCE standardized equations. University of Idaho www.kimberly.uidaho.edu/ref-et
- Allen RG, Pereira LS, Raes D, Smith M (1998) Crop evapotranspiration-Guidelines for computing crop water requirements-FAO Irrigation and drainage paper 56. FAO, Rome, 300(9), D05109
- Allen RG, Walter IA, Elliott RL, Howell TA, Itenfisu D, Jensen ME, Snyder RL (2005) The ASCE standardized reference evapotranspiration equation, Am Soc of Civ Eng Reston, Va
- Ambas VT, Baltas E (2012) Sensitivity analysis of different evapotranspiration methods using a new sensitivity coefficient. *Global NEST J* 14(3):335–343
- Angstrom A (1924) Solar and terrestrial radiation. Report to the international commission for solar research on actinometric investigations of solar and atmospheric radiation. *Q J R Meteorol Soc* 50(210):121–126
- Babst F, Mueller RW, Hollmann R (2008) Verification of NCEP reanalysis shortwave radiation with mesoscale remote sensing data. *IEEE Geosci Remote Sens Lett* 5(1):34–37
- Bakhtiari B, Liaghat AM (2011) Seasonal sensitivity analysis for climatic variables of ASCE-Penman-Monteith model in the semi-arid climate. *J Agric Sci Technol* 13(Supplementary Issue):1135–1145
- Barkstrom BR, Smith GL (1986) The earth radiation budget experiment: science and implementation. *Rev Geophys* 24(2):379–390
- Barkstrom B, Harrison E, Smith G, Green R, Kibler J, Cess R (1989) Earth radiation budget experiment (ERBE) archival and April 1985 results. *Bull of the Am Meteorol Soc* 70(10):1254–1262
- Barkstrom BR, Harrison EF, Lee RB (1990) Earth radiation budget experiment. *Eos, Trans Am Geophys Un* 71(9):297–304
- Betts AK, Chen F, Mitchell KE, Janjić ZI (1997) Assessment of the land surface and boundary layer models in two operational versions of the NCEP eta model using FIFE data. *Mon Weather Rev* 125(11):2896–2916
- Blaney HF, Criddle, W D (1950) Determining water requirements in irrigated area from climatological irrigation data, US Department of Agriculture, soil conservation service, Tech. Pap. No. 96, 48 pp.
- Bojanowski JS (2013) Quantifying solar radiation at the earth surface with meteorological and satellite data. Dissertation, University of Twente
- Bojanowski JS, Vrieling A, Skidmore AK (2013) Calibration of solar radiation models for Europe using Météosat second generation and weather station data. *Agric and For Meteorol* 176:1–9
- Cano D, Monget JM, Albuisson M, Guillard H, Regas N, Wald L (1986) A method for the determination of the global solar radiation from meteorological satellite data. *Sol Energ* 37(1):31–39
- Chen F, Mitchell K, Schaake J, Xue Y, Pan HL, Koren V, Betts A (1996) Modeling of land surface evaporation by four schemes and comparison with FIFE observations. *J Geophys Res: Atmos* 101(D3):7251–7268
- Dai Y, Zeng X, Dickinson RE, Baker I, Bonan GB, Bosilovich MG, Oleson KW (2003) The common land model. *Bull Am Meteorol Soc* 84(8):1013–1023
- Derber JC, Parrish DF, Lord SJ (1991) The new global operational analysis system at the National Meteorological Center. *Weather Forecast* 6(4):538–547
- Duffie JA, Beckman WA (1980) Solar engineering of thermal processes, 1st edn. Wiley, New York
- Duffie JA, Beckman WA (1991) Solar engineering of thermal processes, 2nd edn. Wiley, New York

- Duvel JP, Viollier M, Raberanto P, Kandel R (2001) The ScaRaB-Resurs earth radiation budget dataset and first results. *Bull Am Meteorol Soc* 82(7):1397–1408
- Dybbroe A, Thoss A, Karlsson KG (2000a) The AVHRR & AMSU/MHS products of the Nowcasting SAF. In *Proceedings of the 2000 Eumetsat Meteorological Satellite Data Users' Conference*, Bologna, Italy (pp. 729–736)
- Dybbroe A, Karlsson KG, Moberg M, Thoss A (2000b) A scientific report for the SAFNWC mid-term review, issue 1.1. SMHI, september
- Ek MB, Mitchell KE, Lin Y, Rogers E, Grunmann P, Koren V, Tarpley JD (2003) Implementation of Noah land surface model advances in the National Centers for environmental prediction operational mesoscale eta model. *J Geophys Res: Atmos* 108(D22)
- Gong L, Xu CY, Chen D, Halldin S, Chen YD (2006) Sensitivity of the penman–Monteith reference evapotranspiration to key climatic variables in the Changjiang (Yangtze River) basin. *J Hydrol* 329(3):620–629
- Goyal RK (2004) Sensitivity of evapotranspiration to global warming: a case study of arid zone of Rajasthan (India). *Agri Water Manag* 69(1):1–11
- Gueymard CA, Myers DR (2008) Validation and ranking methodologies for solar radiation models. In: *Modeling solar radiation at the Earth's surface*. Springer, pp. 479–509
- Guitjens JC (1982) Models of alfalfa yield and evapotranspiration. *J Irrig Drain Divis* 108(3):212–222
- Harbeck GE Jr (1962) A practical field technique for measuring reservoir evaporation utilizing mass-transfer theory. *US Geol Surv Paper* 272-E:101–105
- Hargreaves GH, Samani ZA (1982) Estimating potential evapotranspiration. *J Irrig Drain Div* 108(3):225–230
- Hargreaves GH, Samani ZA (1985) Reference crop evapotranspiration from temperature. *Appl Eng Agriculture* 1(2):96–99
- Harries JE, Russell JE, Hanafin JA, Brindley H (2005) The geostationary earth radiation budget project. *Bull Am Meteorol Soc* 86(7):945–960
- Hollmann R, Mueller RW, Gratzki A (2006) CM-SAF surface radiation budget: first results with AVHRR data. *Adv Sp Res* 37(12):2166–2171
- Inamdar AK, Guillevic PC (2015) Net surface shortwave radiation from GOES imagery—product evaluation using ground-based measurements from SURFRAD. *Remote Sens* 7(8):10788–10814
- Jacobowitz H, Tighe RJ (1984) The earth radiation budget derived from the NIMBUS 7 ERB experiment. *J Geophys Res: Atmos* 89(D4):4997–5010
- Jensen ME (1985) Personal communication. ASAE National Conference, Chicago, IL
- Jensen ME, Burman RD, Allen RG (1990) Evapotranspiration and irrigation water requirements. ASCE
- Kalnay E, Kanamitsu M, Kistler R, Collins W, Deaven D, Gandin L, Zhu Y (1996) The NCEP/NCAR 40-year reanalysis project. *Bull Am Meteorol Soc* 77(3):437–471.425
- Kandel R, Viollier M, Raberanto P, Duvel JP (1998) The ScaRaB earth radiation budget dataset. *Bull Am Meteorol Soc* 79(5):765–783
- Kistler R, Collins W, Saha S, White G, Woollen J, Kalnay E, van den Dool H (2001) The NCEP–NCAR 50–year reanalysis: monthly means CD-ROM and documentation. *Bull Am Meteorol Soc* 82(2):247–267
- Koren V, Schaake J, Mitchell K, Duan QY, Chen F, Baker JM (1999) A parameterization of snowpack and frozen ground intended for NCEP weather and climate models. *J Geophys Res: Atm* 104(D16):19569–19585
- Koster RD, Suarez MJ (1992) Modeling the land surface boundary in climate models as a composite of independent vegetation stands. *J Geophys Res: Atmos* 97(D3):2697–2715
- Laszlo I, Ciren P, Liu H, Kondragunta S, Tarpley JD, Goldberg MD (2008) Remote sensing of aerosol and radiation from geostationary satellites. *Adv Sp Res* 41(11):1882–1893
- Liang X, Lettenmaier DP, Wood EF, Burges SJ (1994) A simple hydrologically based model of land surface water and energy fluxes for general circulation models. *J Geophys Res: Atmos* 99(D7):14415–14428
- Liang S, Zhong B, Fang H (2006) Improved estimation of aerosol optical depth from MODIS imagery over land surfaces. *Remote Sens Environ* 104(4):416–425
- Liu X, Li Y, Zhong X, Zhao C, Jensen JR, Zhao Y (2014) Towards increasing availability of the Ångström–Prescott radiation parameters across China: spatial trend and modeling. *Energy Convers Manag* 87:975–989
- Ohmura A, Dutton EG, Forgan B, Frohlich C (1998) Baseline surface radiation network (BSRN/WCRP): new precision radiometry for climate research. *Bull Am Meteorol Soc* 79(10):2115–2136
- Paulescu M, Paulescu E, Gravila P, Badescu, V (2013) Solar radiation measurements. In *weather modeling and forecasting of PV systems operation* (pp. 17–42). Springer London
- Penman HL (1948) Natural evaporation from open water, bare soil and grass. *Proc Royal Soc London A: Math, Phys Eng Sci* 193(1032):120–145
- Piri J, Kisi O (2015) Modelling solar radiation reached to the earth using ANFIS, NN-ARX, and empirical models (case studies: Zahedan and Bojnurd stations). *J Atmos Sol-Terr Phys* 123:39–47
- Priestley CHB, Taylor RJ (1972) On the assessment of surface heat flux and evaporation using large-scale parameters. *Mon Weather Rev* 100(2):81–92

- Rodell M, Houser PR, Jambor UEA, Gottschalck J (2004) The global land data assimilation system. *Bull Am Meteorol Soc* 85(3):381–394
- Rosenberg NJ, Blad BL, Verma, SB (1983) *Microclimate: the biological environment*. John Wiley & Sons
- Samani Z, Bawazir AS, Bleiweiss M, Skaggs R, Tran VD (2007) Estimating daily net radiation over vegetation canopy through remote sensing and climatic data. *J Irrig Drain Eng* 133(4):291–297
- Schulz J, Albert P, Behr HD, Caprion D, Deneke H, Dewitte S, Hollmann R (2009) Operational climate monitoring from space: the EUMETSAT satellite application facility on climate monitoring (CM-SAF). *Atmos Chem Phys* 9(5):1687–1709
- Shapiro R (1972) Simple model for the calculation of the flux of solar radiation through the atmosphere. *Appl Opt* 11(4):760–764
- Sharifi A, Dinpashoh Y (2014) Sensitivity analysis of the penman-monteith reference crop evapotranspiration to climatic variables in Iran. *Water Resour Manag* 28(15):5465–5476
- Wang K, Wang P, Li Z, Cribb M, Sparrow M (2007) A simple method to estimate actual evapotranspiration from a combination of net radiation, vegetation index, and temperature. *J Geophys Res: Atmos* 112(D15)
- Wang F, Wang L, Koike T, Zhou H, Yang K, Wang A, Li W (2011) Evaluation and application of a fine-resolution global data set in a semiarid mesoscale river basin with a distributed biosphere hydrological model. *J Geophys Res: Atmos* 116(D21)
- Xu CY, Singh VP (2002) Cross-comparison of empirical equations for calculating potential evapotranspiration with data from Switzerland. *Water Resour Manag* 16(3):197–219
- Zhang H, Pu Z (2010) Beating the uncertainties: ensemble forecasting and ensemble-based data assimilation in modern numerical weather prediction. *Adv in Meteorol* 2010